Journal of The Electrochemical Society, **163** (2) A251-A254 (2016)
0013-4651/2016/163(2)/A251/4/$33.00 © The Electrochemical Society

High-Capacity and Highly Reversible Silicon-Tin Hybrid Anode for Solid-State Lithium-Ion Batteries

Justin M. Whiteley, Ji Woo Kim,[a] Daniela Molina Piper, and Se-Hee Lee[*,z]

Department of Mechanical Engineering, University of Colorado at Boulder, Boulder, Colorado 80300-0427, USA

This study presents a proof-of-concept: pairing high capacity anode materials by imbedding silicon (Si) in a tin (Sn) matrix. By doing so, a cell is presented with a reversible capacity of 700 mAh g^{-1} (normalized to electrode) for 50 cycles. Through electrochemical analyses and XRD, it is confirmed that Sn is heavily utilized and the extent of Si utilization is calculated. With Sn lithiating prior to Si, an in situ pressure is formed that acts conformally on Si leading to greater reversibility. This study lays the groundwork investigating new architectures to better encapsulate Si in Sn.

Manuscript submitted September 24, 2015; revised manuscript received November 9, 2015. Published November 19, 2015.

Batteries constructed using ceramic electrolytes have become an attractive conception due to enhanced safety and elevated temperature operation.[1] However, new sets of engineering challenges arise when integrating next-generation battery materials into the solid-state; hindrances such as solid electrolyte interphases (SEI) are replaced with solid-solid material interfacing.[2] To enable the use of most energy-dense materials in the solid-state, new tactics must be taken that deviate from the standard battery construction methodology.

Silicon (Si) is the most sought after anode alloying material due to its high theoretical capacity and natural abundance. However, the drawbacks (massive expansion, mechanical pulverization, active material isolation) have also been well documented and studied extensively in the solid-state.[3,4] Molina Piper et al. studied the effect of confinement pressure on silicon: it was concluded that with greater confinement pressure, silicon alloys with fewer moles of lithium than free energy allows while being able to cycle for much longer periods of time.[5] Son et al. and subsequently Yersak et al. applied this concept to confining silicon in a silicon-titanium-nickel (STN) matrix to limit the extent of lithiation while improving reversibility.[3,6] STN is a rather weak mixed conductor with small electrochemical activity and improvements can be made to this concept.

We recently reported on an in situ derived tin (Sn) networked anode.[7] As Sn is ductile and an excellent mixed conductor, long-range interfaces were developed between Sn and solid electrolyte lowering interfacial resistance. The high electrical conductivity absolved the need for carbon additives and therefore prevented active material isolation. Sn additionally does not exhibit any decomposition with the sulfide solid electrolyte (SSE) which allows for superior stability. Sn therefore appears to be a perfect active and mixed conductive matrix to host Si. Only one other study has been identified using this pairing[8] but this was performed in a thin-film format whereas we envision the Sn-Si system as a bulk anode exhibiting commercial grade capacities. For the reasons outlined above, this system does not lend itself to the non-aqueous, solvent based lithium ion system but is better suited for a ceramic-based system.

In this study, we present a proof-of-concept pairing the highest capacity anode material, Si, within a Sn matrix. As Sn lithiates at greater voltages than Si, the pressure derived by Sn's lithiation expansion is used to confine silicon achieving greater reversibility. Thus a solid-state battery is presented with tremendous stability over 50 cycles. Through an extensive electrochemical analyses and X-ray diffraction (XRD), we confirm full utilization of Sn and determine the extent of Si utilization. By replacing some of the more expensive Sn with Si, we present a more commercially viable anode with greater volumetric and gravimetric capacities than previous reports.

Experimental

All procedures outlined were conducted in a dry argon environment. To assemble test cells, a 150 mg glass solid electrolyte pellet separator was first pressed at 1 metric ton inside a polyetheretherketone (PEEK) lined Ti test cell die.[5] The $77.5Li_2S$-$22.5P_2S_5$ glass SSE[9] used as the basis for all-solid-state construction was prepared by ball milling with an appropriate ratio of Li_2S (Aldrich, 99.9%, reagent grade) and P_2S_5 (Aldrich, 99%) using a planetary ball mill (MTI Corporation SFM-1). The composite electrode was a 52.5:17.5:30 weight ratio of Sn powder (100 nm, Alfa Aesar, 99.8%), Si powder (50 nm, Alfa Aesar, 99.99%), and glass SSE mixed by hand with agate mortar and pestle. Thus a 3:1 weight ratio of Sn to Si is used which is approximately a 1:1 volume ratio. 3 mg of the composite electrode was then pressed to one side of the glass electrolyte pellet at 375 MPa. A lithium-indium alloy (stoichiometry of $Li_{0.5}In$) (FMC Lithium Corp., Lectro Max Powder 100 and Indium powder, Alfa Aesar, Puratronic 99.999%) was attached to the opposite side of the pellet as a counter electrode at 375 MPa. The $Li_{0.5}In$ alloy has a potential of 0.62 V versus Li^+/Li for a limited composition range[10] so voltage profile figures are given with respect to Li metal for convenience. Cells are held under 20 MPa during operation. Electrochemical performances were tested using Arbin BT2000 battery test station with a CCCV operation to cycle the cells at 60°C.

To analyze the microstructure, a cell prepared as above was discharged to 5 mV then extruded from the die. XRD was carried out by sealing the pellet in an acrylic holder under a beryllium window to prevent air exposure. XRD patterns were collected with Cu K_α radiation ($\lambda = 1.5418$ Å) in the 2θ range of 20°−60°, using a Bruker AXS D2 Phaser benchtop XRD system operated at 30 kV and 30 mA. A Lynxeye XE 1D detector with a step size of 0.02° and collection time of 1 s per step were employed. Sample displacement was corrected by using a pure corundum internal standard.

Results and Discussion

Figure 1a shows the excellent reversibility of the Sn-Si system over 50 cycles. The cell achieves an active material specific capacity of over 1000 mAh g^{-1}. This is in comparison to the 800 mAh g^{-1} previously achieved with using pure Sn as the anode.[7] The extra capacity clearly comes from the utilization of Si as is confirmed in the voltage profile in Figure 1b. The Si contribution is most evident on the first cycle lithiation and contributes consistently to the remaining cycles. An ideal anode for high energy applications should have as low of a voltage versus lithium as possible. Using pure Sn, we previously achieved a stable cycling anode with an average delithiation voltage of 0.79 V (vs. Li), however, the addition of the silicon lowers the voltage to 0.53 V (vs. Li) which is even more desirable. A coulombic efficiency greater than 100% is evident over the course of cycling. This is attributed to the voltage hold applied at full delithiation and is apparent in Figure 1b.

*Electrochemical Society Active Member.
[a]Present address: Battery Research & Development Division, LG Chem Research Park, Daejeon, 305-738, Korea.
[z]E-mail:sehee.lee@colorado.edu

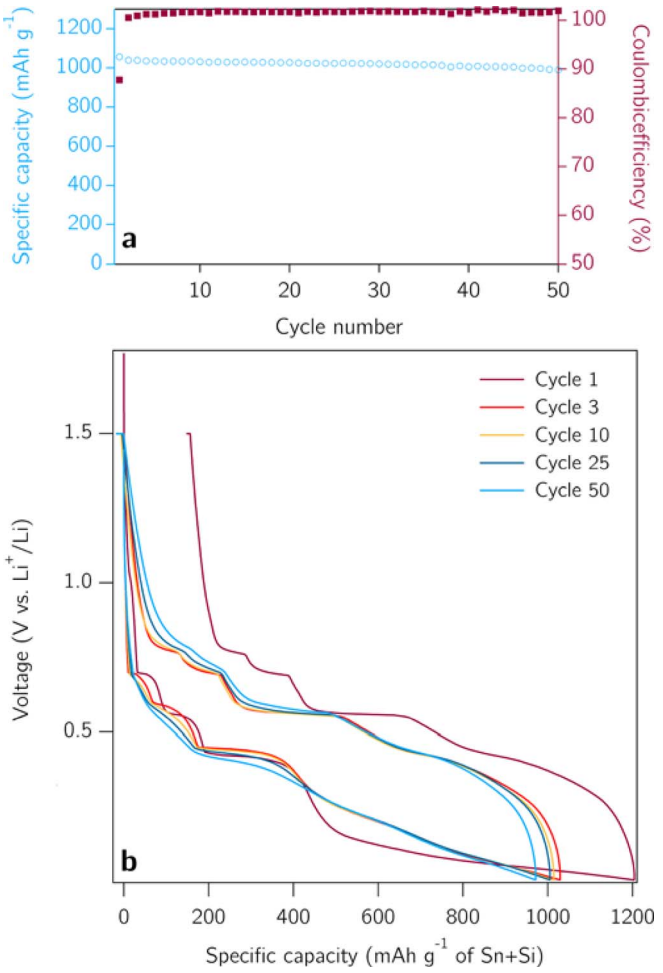

Figure 1. (a) Cycle performance and coulombic efficiency of Sn:Si:SSE [7(3:1):3] anode in an all-solid-state Li-ion battery at 60°C with a C/20-rate (80 mA g^{-1}) and (b) Corresponding voltage profiles of the Sn:Si:SSE anode vs. LiIn counter electrode (converted to vs. Li).

Deconvolution of the system to attribute individual capacities to the different materials can prove tough. Si has a varying voltage profile between the first and subsequent cycles and Sn has five distinct voltage regions. Therefore, cycles 1 and 3 are deconvoluted separately. Distinctive lithiation voltage regions have been assigned using the designation of cycle#-material-region (ie. 1-Si-1 or 3-Sn-4). Figures 2a and 2b are the first and third cycle voltage profiles, respectively, of a Si cell in solid-state.[5] These cells used small mass loadings of Si to achieve good stability thus it is assumed that full utilization of Si occurred. The system clearly represents the Si characteristic: the first cycle contains a single region (1-Si-1) which reflects Si's initial two-phase lithiation where the crystalline Si is consumed to form lithiated amorphous (Li_xSi), the third cycle contains two unique regions (3-Si-1, 3-Si-2) which correspond to amorphous Li_xSi-alloys (the structural changes responsible for these peaks are not clearly understood yet, but thought to be a result of short-range ordering in the amorphous Li_xSi).[11] Figures 2c and 2d are the first and third cycle voltage profiles, respectively, of a Sn cell in solid-state.[7] Sn retains a relatively well-ordered voltage profile from the first to the third cycle. The four distinct regions (1-Sn-1 to 1-Sn-4) represent changes through 7 distinct crystallographic phases culminating in the highest lithiated phase, $Li_{17}Sn_4$.[12] Lastly Figures 2e and 2f are the first and third cycle voltage profiles, respectively, of the Sn-Si hybrid cell under study. The Si and Sn voltage regions have been overlaid onto the profile as well as the differential capacity plotted alongside for convenience. All cells run in Figure 2 use a similar current density per unit mass (approximately 100 mA g active^{-1}) and temperature of operation (60°C) therefore, they are all comparable. Interestingly, the Sn regions exhibit an overpotential on the first cycle (depicted as η_1, η_2, η_3, η_4 in Figure 2e) compared to the pure Sn cell. This is most likely due to the addition of Si preventing free initial expansion. By the third cycle, however, the Sn regions in the Sn-Si cell overlap exactly with the pure Sn. The contribution of the Si is clear in the hybrid cell not just by the increased capacity of the system but its unique print in the voltage profile. Similar to the Sn, Si exhibits a small overpotential (η_5) of about 75.3 mV. This will be explained in the upcoming section. By the third cycle this overpotential nearly disappears except for the lower lithiation voltage which maintains a constant overpotential (η) throughout the cycling of the cell enabling a remarkably reversible Si material. This is the result of a constant external pressure on Si imposed by the active and expanding Sn during its lithiation.[5]

In order to fully determine the extent at which Si is utilized, we examine how much Sn is lithiated. Figure 3 shows the XRD pattern of a hybrid cell which has been discharged to 5 mV [galvanostatic equivalent to the parameters in Figures 1 and 2 (C/20 rate)]. The distinct peaks at 22.1°, 23.5°, and 38.9° (2θ) are attributed to $Li_{17}Sn_4$.[13] Smaller peaks at 32.5°, 37.4°, and 39.7° (2θ) also pertain to the fingerprint of such phase. Facile kinetics of solid state phase transformation allow for this fully lithiated phase to be achieved at room temperature.[14] In our earlier work on the Sn system, we achieved theoretical capacity on the first lithiation.[7] We therefore assume the full lithiation and utilization of the Sn matrix in the hybrid composite anode. Backing out the theoretical capacity of Sn from the actual achieved capacity, we determine that Si alloys with approximately 2.3 mol of Li. Although in this range Si should typically be found in the *a*-Li_xSi alloy,[15] unspecified peaks in Figure 3 fit remarkably well with the Li_7Si_3 phase typically only present at high temperatures.[16] The solid-state amorphization of Si has been proposed many times to be caused by the high nucleation barrier caused by the high interfacial energy.[11,17] Indeed the activation energy for the thermodynamically stable crystalline Li_xSi phases is quite high.[18] Only one study has investigated the effect of compressive stress on silicon alloy dynamics[5] but did not investigate how this impacted nucleation kinetics. Since this hybrid system has Sn, which expands prior to Si lithiation (an expansion on the order of 200% by this stage[7]), an enormous pressure is exerted on Si. This manifests itself as a large strain energy or elastic energy in homogeneous nucleation theory.[19] Thus we propose volumetric barriers overtake interfacial barriers as the limiting factor in the formation of the Li_xSi alloy. In this case, the molar volume of Li_7Si_3 is less than that of the molar volume of *a*-Li_7Si_3 and therefore is preferential. The presence of an initial 75 mV overpotential (η_5) could indicate the additional driving force for silicon crystallization. Unfortunately, this is not an ideal system to study this effect due to the heterogeneity of the electrode. Therefore, we propose to study further this effect by encapsulating Si with Sn to provide a system that can be modeled. Future work will focus on expanding this theory. There is also the possibility that the externally applied pressure required for solid-state battery operation could be playing a role in the crystalline Si phases observed. Although no solid-state work has ever observed this Si behavior before, further work will need to confirm that this is not the case.

If we continue to make the assumption that Sn is fully lithiated throughout cycling, then we can back out the amount of silicon utilization throughout the course of the 50 cycles. Figure 4 presents the extent of Si lithiation. While Sn is most likely not achieving full lithiation every cycle, it is impossible to confirm the exact utilization value as the highest lithiation stages of Sn overlaps with Si. Therefore, our values in Figure 4 are quite conservative. The excellent reversibility of moles of lithium inserted into Si is far greater than our previous report.[5] Previously, we found similar moles of lithium to alloy with Si but using small and external compressive stresses. However, poor stability was shown most likely as compression was applied uniaxially. The inherent stability in this new hybrid can therefore be attributed to the much more uniform application of stress to all sides of the silicon

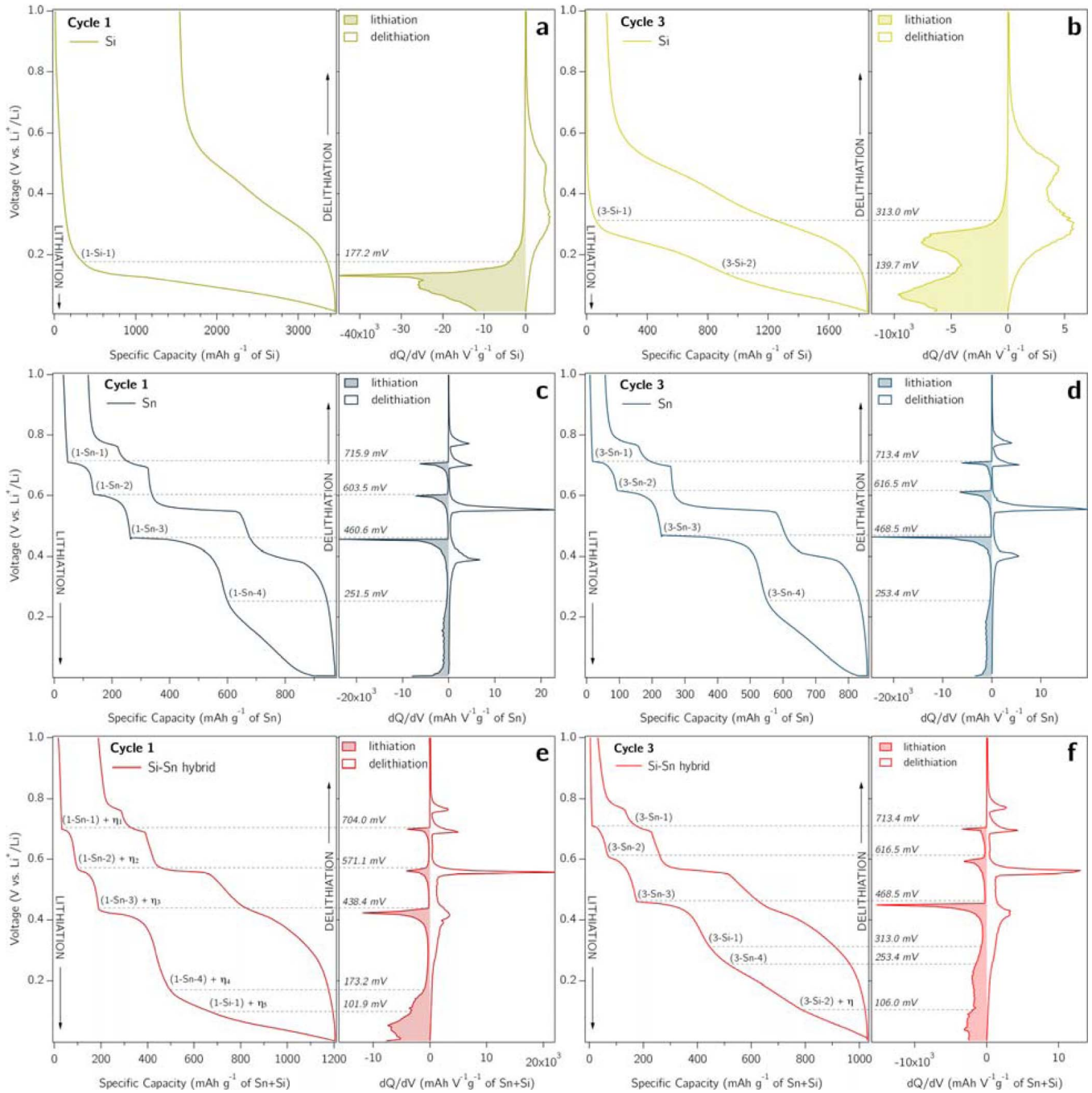

Figure 2. Si anode in solid-state voltage profiles and corresponding dQ/dV spectrum for the first cycle (a), and third cycle (b). Sn anode in solid-state voltage profiles and corresponding dQ/dV spectrum for the first cycle (c), and third cycle (d). Sn:Si hybrid anode in solid-state voltage profiles and corresponding dQ/dV spectrum for the first cycle (e), and third cycle (f). Distinct lithiation regions are assigned for (a) through (d) and overlapped onto (e) and (f). Overpotentials η_1 through η_5 present a hindrance to the volumetric expansion in Sn [e] but disappear once Si has fully amorphized [f].

particles. As this appears to be the case, we propose further work to investigate even better methods of encapsulating Si in Sn such as sputtering, atomic layer deposition, or sol-gel methods.

Conclusions

This study presents a proof-of-concept idea of pairing high capacity anode materials, Sn and Si together. By doing so, we present a cell with a reversible capacity of 700 mAh g^{-1} (normalized to electrode) for 50 cycles. This is a substantial increase from previous work which already demonstrated some of the best performance characteristics of any anode in solid-state to date. We confirm through electrochemical analyses and XRD that Sn is fully utilized and calculate the extent of Si utilization. With Sn lithiating prior to Si, we create an in situ pressure that acts conformally on Si. Therefore we achieve greater extent of lithiation and better reversibility than our previous studies using uniaxial pressure for reversible Si alloying. The idea of using Sn as a mixed conductive, electrochemically active matrix to imbed Si is a new concept. New architectures will be investigated further to get better encapsulation of Si.

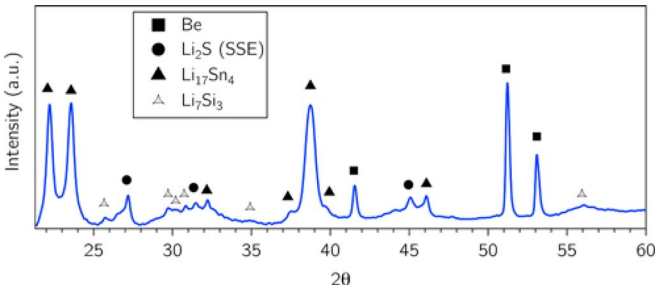

Figure 3. (a) Ex-situ XRD spectrum of Sn:Si:SSE anode discharged to 5 mV vs. Li. Sn fully lithiates to $Li_{17}Sn_4$ phase. In-situ derived pressure from Sn expansion allows Si to crystallize to the Li_7Si_3 phase rather than remaining in the amorphous analogue.

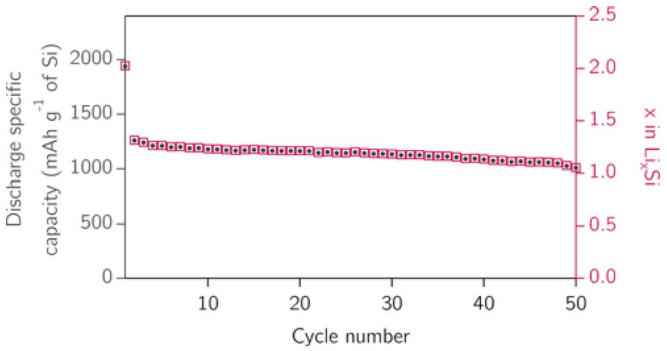

Figure 4. Moles of Li per Si or specific capacity of Si in the Sn:Si:SSE anode in Figure 1. The value is developed assuming Sn fully lithiates every cycle.

Acknowledgments

This material is based on research sponsored by Air Force Research Laboratory under agreement number FA9453-15-1-0304. The U.S. Government is authorized to reproduce and distribute reprints for Governmental purposes notwithstanding any copyright notation thereon.

References

1. J. W. Fergus, *Journal of Power Sources*, **195**, 4554 (2010).
2. T. A. Yersak, T. Evans, J. M. Whiteley, S. B. Son, B. Francisco, K. H. Oh, and S. H. Lee, *Journal of the Electrochemical Society*, **161**, A663 (2014).
3. S. B. Son, S. C. Kim, C. S. Kang, T. A. Yersak, Y. C. Kim, C. G. Lee, S. H. Moon, J. S. Cho, J. T. Moon, K. H. Oh, and S. H. Lee, *Advanced Energy Materials*, **2**, 1226 (2012).
4. J. E. Trevey, K. W. Rason, C. R. Stoldt, and S. H. Lee, *Electrochemical and Solid State Letters*, **13**, A154 (2010).
5. D. M. Piper, T. A. Yersak, and S. H. Lee, *Journal of the Electrochemical Society*, **160**, A77 (2013).
6. T. A. Yersak, S. B. Son, J. S. Cho, S. S. Suh, Y. U. Kim, J. T. Moon, K. H. Oh, and S. H. Lee, *Journal of the Electrochemical Society*, **160**, A1497 (2013).
7. J. M. Whiteley, J. W. Kim, C. S. Kang, J. S. Cho, K. H. Oh, and S.-H. Lee, *Journal of the Electrochemical Society*, **162**, A711 (2015).
8. T. D. Hatchard and J. R. Dahn, *Journal of the Electrochemical Society*, **151**, A1628 (2004).
9. T. A. Yersak, H. A. Macpherson, S. C. Kim, V. D. Le, C. S. Kang, S. B. Son, Y. H. Kim, J. E. Trevey, K. H. Oh, C. Stoldt, and S. H. Lee, *Advanced Energy Materials*, **3**, 120 (2013).
10. K. Takada, N. Aotani, K. Iwamoto, and S. Kondo, *Solid State Ionics*, **86–8**, 877 (1996).
11. W.-J. Zhang, *Journal of Power Sources*, **196**, 877 (2011).
12. I. A. Courtney, J. S. Tse, O. Mao, J. Hafner, and J. R. Dahn, *Physical Review B*, **58**, 15583 (1998).
13. G. R. Goward, N. J. Taylor, D. C. S. Souza, and L. F. Nazar, *Journal of Alloys and Compounds*, **329**, 82 (2001).
14. J. R. Dahn, I. A. Courtney, and O. Mao, *Solid State Ionics*, **111**, 289 (1998).
15. M. N. Obrovac and L. Christensen, *Electrochemical and Solid State Letters*, **7**, A93 (2004).
16. Y. Wang and J. Dahn, *Journal of the Electrochemical Society*, **153**, A2314 (2006).
17. P. Limthongkul, Y. I. Jang, N. J. Dudney, and Y. M. Chiang, *Journal of Power Sources*, **119**, 604 (2003).
18. V. L. Chevrier, H. M. Dahn, and J. R. Dahn, *Journal of the Electrochemical Society*, **158**, A1207 (2011).
19. F. Abraham, in: *Homogeneous Nucleation Theory*, Academic Press Inc., New York, 1974.